

## AN APPLICATION OF GABIONS FOR DESIGN OF COASTAL PROTECTION STRUCTURES IN LAKES

Raimondas Šadzevičius<sup>1</sup>✉, Dainius Ramukevičius<sup>1</sup>, Raimundas Baublys<sup>1</sup>,  
Wojciech Sas<sup>2</sup>, Andrzej Głuchowski<sup>2</sup>, Luiza Rzepczyńska<sup>2</sup>, Kamil Zajęc<sup>2</sup>

<sup>1</sup>Department of Water Engineering, Vytautas Magnus University Agriculture Academy, Kaunas, Lithuania

<sup>2</sup>Water Center Laboratory, Warsaw University of Life Sciences – SGGW, Warsaw, Poland

### ABSTRACT

With large areas of water reservoirs and lakes, the wave runoff distance is also large, resulting in the high waves in the wind blow direction. These waves intensively disrupt the coast of the lake or water reservoir. Another intense factor of coastal erosion is ice. A lot of engineering measures for the coastal protection of reservoirs and especially for lakes are used: reinforced concrete slabs, blocks, jibs, cellular systems (geosynthetics), etc. An eroded coastline, reshaped by installing a coastal protection structure using gabion construction, is analysed in this research. Gabions are designed to protect banks and slopes from fast water flow (water speed over  $5 \text{ m} \cdot \text{s}^{-1}$ ) and ice impacts. They are designed according to geotechnical principles, assessing stability according to the limit design situations specified in Eurocode 7 (EN 1997-1). The aim of this work is to illustrate the features of wave and ice loads and geotechnical design situations evaluated in the design of a coastal protection structure made of gabions.

**Keywords:** coastal protection structures, waves and ice impacts, gabions, geotechnical design situations

### INTRODUCTION

The coastline shows constantly varying nature due to tidal effects and changes in wind and wave climate. Sediment movement, erosion and accretion are responsible for changing the morphology of coastal area. Human activities/interference is also responsible for changes in the coastline (Kudale, Kudale & Kulkarni, 2021).

With large areas of water reservoirs and lakes, the wave runoff distance is also large, resulting in the high waves in the wind blow direction. These waves intensively disrupt the coast of the lake or water reservoir. The wave forces are dominant and decisive in the design of coastal structures. Structural stability as well as functional performance of

a coastal structure depends on design wave conditions (Kudale & Bhalerao, 2015).

An integrated coastal engineering numerical model is presented by Karambas and Samaras (2017). The model simulates a linear wave propagation, wave-induced circulation, sediment transport and bed morphology evolution. The assessment of wave energy dissipation on the three barriers was executed using two approaches – ordinary dean functions and the concept of monotonic approximate seabed proposed by Różyński (2020) and by Różyński and Cerkowniak (2022). Coastal protection structures influence on diffraction and reflection of waves simulation based on 3D wave hydrodynamics model is presented by Sukhinov, Chistyakov and Protsenko (2021).

Raimondas Šadzevičius <https://orcid.org/0000-0002-7616-6598>; Dainius Ramukevičius <https://orcid.org/0000-0002-9377-7411>;

Raimundas Baublys <https://orcid.org/0000-0003-2218-9214>; Wojciech Sas <https://orcid.org/0000-0002-5488-3297>;

Andrzej Głuchowski <https://orcid.org/0000-0001-6651-6737>; Luiza Rzepczyńska <https://orcid.org/0000-0002-7985-3721>;

Kamil Zajęc <https://orcid.org/0000-0002-5957-9462>

✉ [raimondas.sadzevicius@vdu.lt](mailto:raimondas.sadzevicius@vdu.lt)

Another intense factor of coastal erosion is ice (Łabuz, 2015). Some researchers (Smith & Houser, 2022) think opposite – ice cover reduces erosion during the winter months by limiting fetch across the lake and creating a protective ice foot at the shoreline.

The effect of an ice cover depends on many factors: the length of the ice field, the thickness of the ice, a layer of snow, the temperature of the ice and the rates at which it is expanding and shrinking, the coefficient of friction against the material of the structure and soil, the mechanical properties of the ice and the shape of the water body and structure. An ice cover may exert the following actions against inclined structures: static pressure due to continuous thermal expansion as a result of a temperature rise in the ambient medium, the dynamic effect of floating ice blocks and a breakaway effect when the water level changes.

Coastal protection generally refers to the protection of people, infrastructure and other assets from the negative consequences resulting from flooding (high water levels and/or wave overtopping) and erosion (Möller, 2019). A lot of engineering measures for the coastal protection of reservoirs and especially for lakes are used: reinforced concrete slabs, blocks, jibs, cellular systems (geosynthetics), etc. Dikes may also be constructed from various materials, most commonly: geosynthetic tubes, geo-cells, reinforced concrete, boulders, steel, or gabions (Razali et al., 2023).

Coastal protection based on ecological engineering provides a new concept of resisting coastal zone disasters (Luan, Li, Chen, Geng & Liu, 2020).

Innovative technical solutions for the development of bioengineering systems combined with gabions are presented by Kurbanov, Sozaev, Shogenov & Karshiev (2021).

This paper focuses on coastal protection structure made from gabions. Gabions and mattresses assortment is useful as an integral part of shore fortification and protection, the river bed and slope lining structures. Modern box gabions consist of rockfill material enlaced by a basket or a mesh, shaped like a rectangular box (Chanson, 2015). Gabion type retaining structures constitute one of

the most economical and efficient solutions for stabilization of natural ground slope. Gabion walls are also preferred for the efficiency of the drainage instead of gravity walls. As a construction material, the advantages are their stability, low cost, flexibility and porosity (Toprak, Sevim & Kalkan, 2016).

Gabions are extensively used for earth retaining structures as well as hydraulic structures: retaining walls, bridge abutments, wing walls, culvert headwalls, outlet aprons, shore and beach protection walls, temporary check dams (Cherkasova, 2019).

Gabions participate in the formation of ice conditions and generate icing problems. For example, an ice-stone mass with a certain porosity and strength properties, which creates favourable conditions for the floating and shifting of the gabions, separation from the basic ice mass, interaction with ice layers and attrition by the moving ice, is formed when the gabions are frozen into ice. Structures formed by gabions should be able to resist against different types of ice loads. The artificial measures to increase ice thickness and thin gabion mattress in the context of climate warming were explained by Chunjiang et al. [s.a.].

The assessment of the technical conditions of bank protection in Poznań on hydrotechnical structures are presented by Hämmerling, Walczak, Walczak and Zawadzki (2019).

Numerical modeling of failure mechanisms in articulated concrete block mattress is presented by Safari Ghaleh, Aminoroayaie Yamini, Mousavi and Kavianpour (2021).

The aim of this work is to illustrate the features of wave and ice loads and geotechnical design situations evaluated in the design of a coastal protection structure (made from gabions) in lakes.

The following research tasks were define:

- calculation of the wave and ice loads and evaluation of design situations for design of a gabion retaining wall for shore protection;
- checking the stability of a typical gabion retaining wall in case of overturning and sliding;
- evaluation of the strength of the gabion retaining wall base according the loss of load-bearing capacity.

## MATERIAL AND METHODS

### The object of investigation

Construction site of the designed structure is located in the Meteliai village, Seirijai eldership, Lazdijai district municipality (Fig. 1).

The reinforced concrete retaining wall was installed for shore protection. The existing retaining wall has serious problems: as a result of a washed foundation plate base, the retaining wall has lost stability, settled unevenly and ruptured (Fig. 2).

It is suggested to demolish reinforced concrete retaining wall and replace it by newly designed



**Fig. 1.** The eroded coast of the lake Meteliai

Source: © Geoport.lt.



**Fig. 2.** The deformations and deteriorations of existing reinforced concrete retaining wall

Source: photos by the authors.

retaining wall made of gabions. Gabion elements are preferred because of their flexibility, permeable nature, low costs, environmentally friendliness and aesthetically pleasing nature in comparison with gravity retaining walls (Toprak, Sevim & Kalkan, 2016).

Recycled materials (crushed concrete from existing wall) can be placed into the gabion cage. The use of crushed concrete (large grains) can be applied as filling of mattresses or gabions (Fiske, 2014; Kawalec, Kwiecien, Pilipenko & Rybak, 2017).

### Scheme of retaining wall for shore protection

The coastal protection structure according to Lithuanian Building Technical Regulation STR 1.01.03:2017 (Classification of structures), (Lietuvos Standartizacijos Departamentas, 2017) is classified as hydraulic structures. Coastal protection structures are classified in consequence class CC2 according to Lithuanian Building Technical Regulation STR 2.02.06:2004 (Hydraulic structures. Basic provisions. Annex 1), (Lietuvos Standartizacijos Departamentas, 2004a).

The walls of gabion baskets and grid-stone mattresses with planting will be used as retaining structures for eroded shoreline and bank strengthening. The appropriate filtration materials have to be chosen for gabions so that they protect from washing elements of soil from under the baskets. Geotextile is most commonly used for this purpose (Fig. 3). Engineering infrastructure (coastal protection structure) should be designed and installed with the least possible change in the nature of the landscape and without polluting the environment.

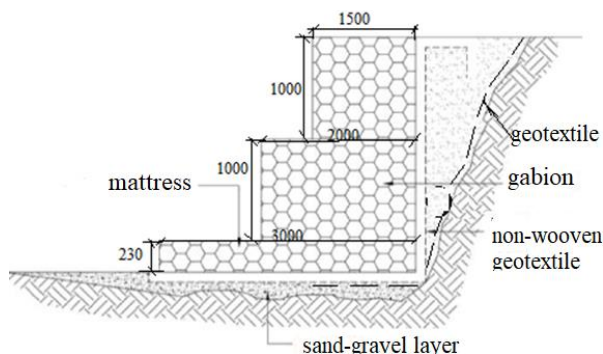


**Fig. 3.** Scheme of retaining wall for shore protection

Source: own work.

### Methodology for calculating loads applicable to coastal protection

The consequence class of hydraulic structures is determined in accordance with Lithuanian Building Technical Regulation STR 2.02.06:2004 (Hydraulic structures. Basic provisions. Annex 1).

Loads acting on the shore protection structure are calculated in accordance with Lithuanian Building Technical Regulation STR 2.05.15:2004 (Effects and loads on hydraulic structures), (Lietuvos Standartizacijos Departamentas, 2004b).

Wave loads are calculated in accordance with Lithuanian Building Technical Regulation STR 2.05.15:2004 (Section X. Wind loads on shore protection structures and ship waves on canal slope protection. Section I. Wind loads on shore protection structures).

The maximum values of the horizontal ( $P_x$ ) and vertical ( $P_z$ ) representative projections of the linear loads from wind-caused waves on the vertical seawall (when the waves roll down) must be determined according to the wave lateral and back pressure graphs (Fig. 4). The value of the pressure ( $p_r$ ), shown in the graphs, must be calculated as follows:

$$p_r = \rho g (\Delta z_r - 0.75h_{br}), \quad (1)$$

where:

$\rho$  – water density [ $\text{kg}\cdot\text{m}^{-3}$ ],

$g$  – gravitational acceleration [ $\text{m}\cdot\text{s}^{-2}$ ],

$\Delta z_r$  – lowering the water level from the calculated water level in front of the vertical wall, when the wave rolls down [m]; it depends on the distance between the structure and the water boundary line:  $\Delta z_r = 0$  when  $a_l \geq 3h_{br}$  and  $\Delta z_r = 0.25h_{br}$  when  $a_l < 3h_{br}$ ,

$h_{br}$  – height of falling waves [m].

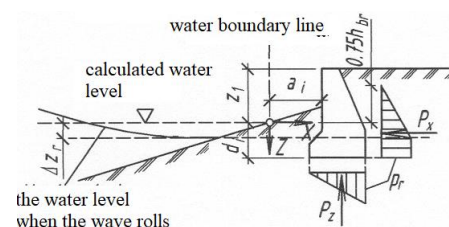


**Fig. 4.** Graphs of the wave pressure on the vertical seawall during the wave rolling down

Source: own work.

Ice loads were calculated in accordance with Lithuanian Building Technical Regulation STR 2.05.15:2004 (Effects and loads on hydraulic structures: Section II. Loads of moving ice fields into structures; Section III. Loads and effects on structures due to thermal expansion of continuous ice cover; Section V. Loads of ice on the structure as the water level changes).

According to the STR 2.05.15:2004, the impact force of moving ice fields in contact with section of structure with a vertical front edge of any shape is calculated in two cases (the lower value is taken for further calculations):

- when it is hit by single ice floes:

$$F_{c,w} = 0.07v h_d \sqrt{AR_c} \text{ [MN]}, \quad (2)$$

- when ice collapses:

$$F_{b,w} = 0.5R_c b h_d \text{ [MN]}, \quad (3)$$

where:

$v$  – ice field movement velocity (determined on the basis of field investigations, and in their absence, as follows: for rivers and flood-exposed sea sections – keeping the flow rate constant; water reservoirs and seas – at a level equal to 0.03 wind velocity, determined during the drifting of the ice with a probability of 1%), [m·s<sup>-1</sup>],

$h_d$  – calculated ice thickness (taken as for rivers – 0.4 m at 1% probability), [m],

$A$  – area of the ice field (determined on the basis of field investigations in the area under consideration or in the vicinity of the water body), [m<sup>2</sup>],

$R_c$  – standard compressive strength of ice [MPa].

When salinity is below 2‰, then the linear load resulting from a thermal expansion ( $q$ ) of the ice cover should be calculated as follows

$$q = h_{\max} k_l p_t, \quad (4)$$

where:

$h_{\max}$  – maximum ice cover thickness at 1% probability [m],

$k_l$  – coefficient equal to 1 [–],

$p_t$  – pressure of deformation of the ice expanding due to temperature changes [MPa]:

$$p_t = 0.05 + 11 \cdot 10^{-5} v_{t,a} \eta_i \mu, \quad (5)$$

where:

$v_{t,a}$  – maximum rate of air temperature rise (from 6 h of four-timed observations) [°C·h<sup>-1</sup>],

$\eta_i$  – coefficient of ice creep [MPa·h<sup>-1</sup>], calculated according to the formulas:

$$\text{when } t_i \geq -20^\circ\text{C}, \quad \eta_i = (3.3 - 0.28 t_i + 0.083 t_i^2) 10^2; \quad (6)$$

$$\text{when } t_i < -20^\circ\text{C}, \quad \eta_i = (3.3 - 1.85 t_i) 10^2; \quad (7)$$

$t_i$  – ice temperature [°C], calculated as follows:

$$t_i = t_b h_{\text{rel}} + 0.5 v_{t,a} \cdot t \cdot \psi, \quad (8)$$

where:

$t_b$  – initial air temperature from which the temperature rise begins [°C],

$h_{\text{rel}}$  – relative thickness of the ice cover, taking into account the influence of snow:

$$h_{\text{rel}} = h_{\max} / h_{\text{red}}, \quad (9)$$

where:

$h_{\text{red}}$  – reduced thickness of the ice cover, calculated as follows:

$$h_{\text{red}} = h_{\max} + 1.43 h_{s,\min} + 2.3/\alpha, \quad (10)$$

where:

$h_{s,\min}$  – minimum thickness of the snow cover, determined by natural observations; if there is no snow,  $h_{s,\min} = 0$  is taken,

$\alpha$  – heat transfer coefficient of air and snow cover [W·m<sup>-2</sup>],

$$\text{if there is snow, then } \alpha = 23 \sqrt{v_{w,m} + 0.3}, \quad (11)$$

where:

$v_{w,m}$  – average wind speed [m·s<sup>-1</sup>],

$\psi, \varphi$  – dimensionless coefficients determined by  $h_{\text{rel}}$  and the dimensionless parameter  $F_0$ :

$$F_0 = 4 \cdot 10^3 t / h_{\text{red}}^2 \quad (12)$$

The vertical force of the ice cover frozen to the structure as the water level changes ( $F_d$ ) [MN], (Fig. 5), should be calculated as follows:

$$F_d = 0.2lv_d t_d (h_{\text{max}}^3 / \Phi)^{0.25}, \quad (13)$$

where:

$l$  – length of the static section at the level of ice exposure [m],

$v_d$  – speed of rise or fall of the water level [ $\text{m} \cdot \text{h}^{-1}$ ],

$t_d$  – time during which the deformation of the ice cover occurs when the water level changes [h],

$h_{\text{max}}$  – maximum ice cover thickness at 1% probability [m],

$\Phi$  – dimensionless time function expressed by the formula:

$$\Phi = 1 + 300[t_d + 50(1 - e^{-0.4t_d})] / \eta_i, \quad (14)$$

where:

$\eta_i$  – coefficient of ice creep [ $\text{MPa} \cdot \text{h}^{-1}$ ].

$t_d, e$  – see explained early.

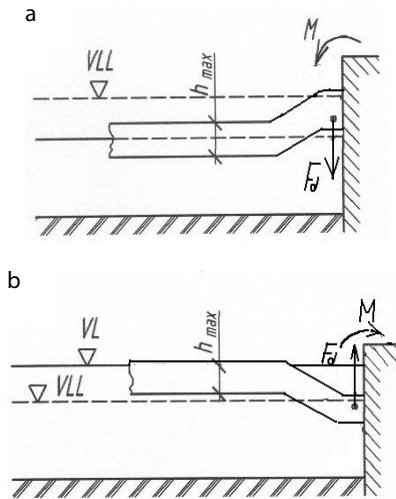


**Fig. 5.** Schemes of the ice cover frozen to the structure loads calculations, when the water level (VL) changes: a – when the VL is falling, b – when the VL is rising; VLL – water level when the ice is standing

Source: STR.2.05.15.2004.

The moment of force ( $M$ ) [ $\text{MN} \cdot \text{m}^{-1}$ ], which is absorbed by the structure from the frozen ice cover when the water level rises or falls (Fig. 5), should be calculated according to the formula:

$$M = 2lv_d t_d \sqrt{h_{\text{max}}^3 / \Phi}, \quad (15)$$

where:

$l, v_d, t_d, h_{\text{max}}, \Phi$  – see explained early.

Note: The limiting force moment ( $M_{\text{lim}}$ ) [ $\text{MN} \cdot \text{m}^{-1}$ ], cannot be greater than this calculated according to the formula:

$$M_{\text{lim}} = 0.167lh_{\text{max}}^2 R_t R_c (1 + 2k_e) / (R_t + R_c), \quad (16)$$

where:

$R_t, R_c$  – tensile and compressive strength of ice cover [MPa], calculated according to the formulas:

$$R_t = R_{t,y} \cdot e^{-400t_{\text{cal}}/\eta}, \quad (17)$$

$$R_c = R_{c,y} \cdot e^{-400t_{\text{cal}}/\eta}, \quad (18)$$

where:

$R_{t,y}, R_{c,y}$  – the average values of the ice yield strength in tension and compression [Pa],

$t_{\text{cal}}$  – the time during which the water level changes by a size equal to the thickness of the ice [h],

$k_e$  – coefficient assuming the following values:

$e^{-400t_{\text{cal}}/\eta}$	0.8	0.85	$\geq 0.90$
$k_e$	1.0	1.5	2.0

$h_{\text{max}}, \eta_i, l$  – see explained early.

Hydrodynamic forces lead further the structural deformations and settlement to geotechnical instability. Failure due to hydrodynamic forces can be avoided by adopting proper dimensions and suitable weight for gabion box (Sherlin, Sundaravadivelu & Saha, 2018).

### Methodology of geotechnical stability analysis

Gabion retaining walls should be designed as mass gravity walls, using standard soil mechanics principles. No allowance should be made for the strength or mass of the wire mesh and the density of the filled gabions should be taken as 60% of the density of the solid rock used.

According to the limit design situations specified in Eurocode 7 (European Union [EU], 2004) the stability should be analysed for: overturning, sliding, bearing failure, localised deformation or failure of the wall and deep seated failure of the retained slope.

Geotechnical stability is analysed numerically using software GEO5 for different loads. The calculation methods for wall analysis:

- active earth pressure calculation: Coulomb,
- passive earth pressure calculation: Caquot–Kerisel,
- earthquake analysis: Mononobe–Okabe,
- shape of earth wedge: calculate as skew,
- allowable eccentricity: 0.333,
- verification methodology: according to EN 1997,
- design approach: 2 – reduction of actions and resistances.

### RESULTS AND DISCUSSION

#### The results of wave loads calculation

With large areas of lake the wave runoff distance is also large, resulting in the high waves in the wind blow direction (Fig. 6). The initial parameters for wave loads calculation are presented in Table 1. The results of wave loads calculation are presented in Table 2.

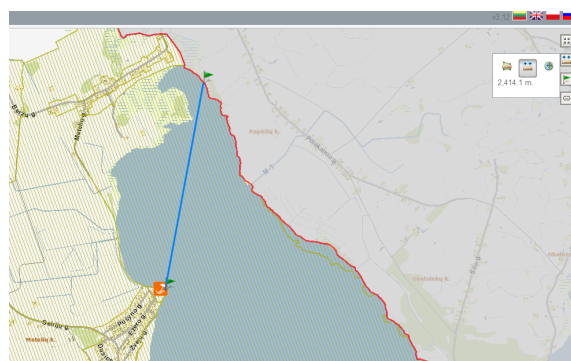


**Fig. 6.** The wave runoff distance

Source: © Geoportal.lt.

**Table 1.** Initial parameters for wave load calculation

Slope angle (acc. to Fig. 4)	0°			10°			15°		
	20	25	30	20	25	30	20	25	30
Wind speed ( $V_w$ ) [ $m \cdot s^{-1}$ ]	20	25	30	20	25	30	20	25	30
Average wave height ( $h$ ) [m]	1.57	1.57	1.72	1.57	1.57	1.72	0.88	1.57	1.72
Average wave length ( $\lambda$ ), m	40.95	41.01	44.68	40.95	41.01	44.68	41.93	41.01	44.68
Average wave period ( $T$ ) [s]	7.86	7.85	8.19	7.86	7.85	8.19	7.86	7.85	8.19
Depth at first wave break ( $d_{cr}$ ) [m]	1.99	2	2.18	1.99	2	2.18	2.11	2	2.18
The depth of the last wave break ( $d_{cu}$ ) [m]	0.62	0.63	0.68	0.62	0.63	0.68	0.66	0.63	0.68
Calculated maximum wave height ( $h_j$ ) [m]	1.57	1.57	1.72	1.57	1.57	1.72	1.67	1.57	1.72
The maximum rise of the wave crest above the calculated level ( $n_w$ ) [m]	1.44	1.45	1.58	1.44	1.45	1.58	1.53	1.45	1.58

Source: own work.

**Table 2.** Wave load calculation results

Slope angle (acc. to Fig. 4)	0°			10°			15°		
	20	25	30	20	25	30	20	25	30
When the waves roll down, the projection of the wave is horizontal ( $P_x$ ) [ $kN \cdot m^{-1}$ ]	6.08	6.13	7	6.08	6.13	7	6.72	6.13	7
Addition point of horizontal load ( $z_1$ ) [m]	-0.12	-0.13	-0.16	-0.12	-0.13	-0.16	-0.15	-0.13	-0.16
When the waves recede, the projection of the wave is vertical (back pressure) ( $P_z$ ) [ $kN \cdot m^{-1}$ ]	7.68	7.72	8.44	7.68	7.72	8.44	8.21	7.72	8.44

Source: own work.

Based on the results of the wave loading calculations, Table 2 shows that the changes of slope angle from  $0^\circ$  to  $15^\circ$  directly affect wave loads calculation results only at wind speed  $V_w = 20 \text{ m}\cdot\text{s}^{-1}$ .

### The results of ice loads calculation

The initial parameters for ice loads calculation are presented in Table 3. The results of ice loads (Figs 5 and 7) calculation are presented in Table 4.

**Table 3.** Initial parameters for ice loads calculation

Parameter	Value
Ice temperature at the air-ice contact zone ( $T_u$ ) [ $^\circ\text{C}$ ]	5
Ice temperature at the air-ice contact zone during ice movement ( $T_l$ ) [ $^\circ\text{C}$ ]	4
Calculated temperature drop ( $dT$ ) [ $^\circ\text{C}$ ]	5
Ice thickness ( $h_d$ ) [m]	0.4
Maximum area ice field at 1% probability ( $A_l$ ) [ $\text{m}^2$ ]	50
Speed of ice field movement ( $v_l$ ) [ $\text{m}\cdot\text{s}^{-1}$ ]	1
The average snow cover thickness during the calculation period when the temperature drops ( $h_s$ ) [m]	0.2
Average wind speed during the temperature drop ( $V_w$ ) [ $\text{m}\cdot\text{s}^{-1}$ ]	10
Change in water level ( $h_0$ ) [m]	0.4

Source: own work.

For various ice thicknesses (0.3 m, 0.4 m, 0.5 m), variable wind speed ( $10 \text{ m}\cdot\text{s}^{-1}$ ,  $15 \text{ m}\cdot\text{s}^{-1}$ ,  $20 \text{ m}\cdot\text{s}^{-1}$ ), variable speed of ice field movement ( $0.5 \text{ m}\cdot\text{s}^{-1}$ ,  $1 \text{ m}\cdot\text{s}^{-1}$ ,  $1.5 \text{ m}\cdot\text{s}^{-1}$ ), change in water level (0.3, 0.4 and 0.5 m) as well as various ice field areas ( $50 \text{ m}^2$ ,  $100 \text{ m}^2$ ,  $150 \text{ m}^2$ ), the following ice loads have been calculated: 1) the impact force of moving ice fields in contact with structure [ $P_1$  or  $F_{b,w}$  – Eq. (3)]; 2) ice impact due to the temperature expansion of the continuous ice cover ( $P_3$  or  $q$  – Eq. (4)); 3) the vertical force [ $P_6$  or  $F_d$  – Eq. (13)] and moment [ $M_1$  or  $M$  – Eq. (15)] of the ice frozen on the structure, with the changing water level. The results of the calculations are presented in Table 4.

Based on the results of the ice loading calculations, Table 4 shows that the changes of ice thickness directly affect calculation results of all types of the ice loads. The changes of average wind speed during the temperature drop ( $V_w$ ) have impact on values of horizontal linear loads on structures due to ice cover thermal expansion effect ( $P_3$  or  $q$ ). The changes of speed of ice field movement ( $v_l$ ) from  $0.5 \text{ m}\cdot\text{s}^{-1}$  to  $1.5 \text{ m}\cdot\text{s}^{-1}$  and ice field maximum area ( $A_l$ ) from  $50 \text{ m}^2$  to  $150 \text{ m}^2$  directly influences calculation results of the horizontal load of moving ice fields on a structure

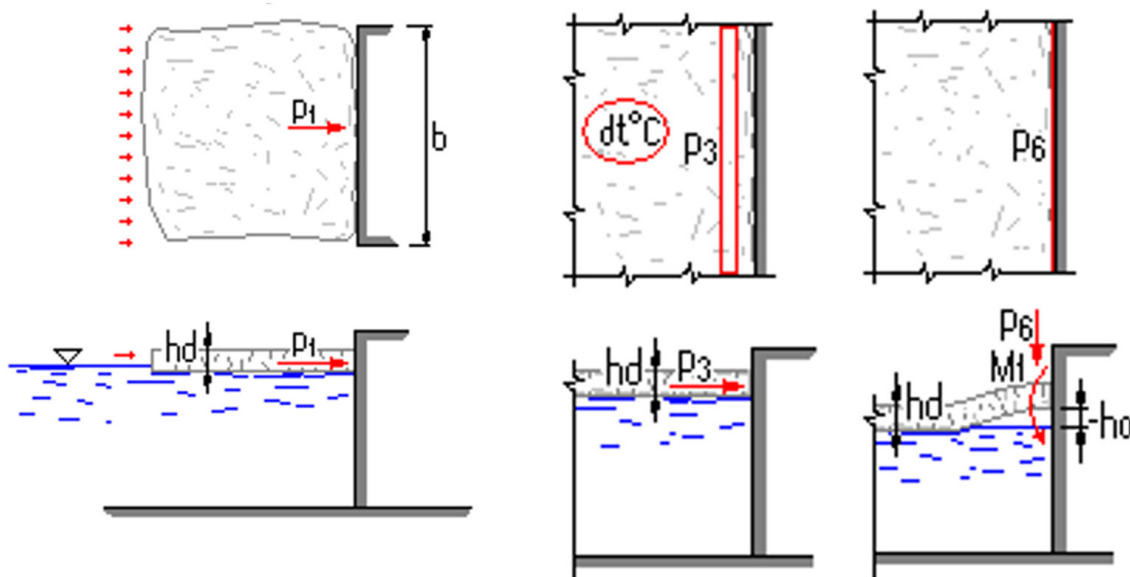


**Fig. 7.** The illustration of ice loads

Source: own work.



**Table 4.** Calculation results of ice loads

Parameter which has been changed	Horizontal load of moving ice fields on a structure with a vertical front edge ( $P_1$ or $F_{b,w}$ ) [kN]	Horizontal linear load on structures due to ice cover thermal expansion effect ( $P_3$ or $q$ ) [ $\text{kN}\cdot\text{m}^{-1}$ ]	Vertical force of the ice cover frozen to the structure as the water level changes ( $P_6$ or $F_d$ ) [ $\text{kN}\cdot\text{m}^{-1}$ ]	Moment absorbed by the structure from the frozen ice cover when the water level rises or falls ( $M_1$ or $M$ ) [ $\text{kNm}\cdot\text{m}^{-1}$ ]
Ice thickness ( $h_d$ ) 0.3 m	131.62	34.6	4.5	19.74
Ice thickness ( $h_d$ ) 0.4 m	175.49	29.2	5.58	35.1
Ice thickness ( $h_d$ ) 0.5 m	219.36	41.4	6.6	54.84
Average wind speed during the temperature drop ( $V_w$ ) $10 \text{ m}\cdot\text{s}^{-1}$	175.49	29.2	5.58	35.1
Average wind speed during the temperature drop ( $V_w$ ) $15 \text{ m}\cdot\text{s}^{-1}$	175.49	35.2	–	35.1
Average wind speed during the temperature drop ( $V_w$ ) $20 \text{ m}\cdot\text{s}^{-1}$	175.49	41.2	5.58	35.1
Speed of ice field movement ( $v_i$ ) $0.5 \text{ m}\cdot\text{s}^{-1}$	118.51	29.2	5.58	35.1
Speed of ice field movement ( $v_i$ ) $1.0 \text{ m}\cdot\text{s}^{-1}$	175.49	29.2	5.58	35.1
Speed of ice field movement ( $v_i$ ) $1.5 \text{ m}\cdot\text{s}^{-1}$	259.63	29.2	5.58	35.1
Change in water level ( $h_0$ ) 0.3 m	175.49	29.2	5.58	35.1
Change in water level ( $h_0$ ) 0.4 m	175.49	29.2	5.58	35.1
Change in water level ( $h_0$ ) 0.5 m	175.49	29.2	5.58	35.1
Maximum area ice field at 1% probability ( $A_i$ ) $50 \text{ m}^2$	175.49	29.2	5.58	35.1
Maximum area ice field at 1% probability ( $A_i$ ) $100 \text{ m}^2$	248.18	29.2	5.58	35.1
Maximum area ice field at 1% probability ( $A_i$ ) $150 \text{ m}^2$	303.96	29.2	5.58	35.1

Source: own work.

with a vertical front edge ( $P_1$  or  $F_{b,w}$ ). In the case of a change in water level ( $h_0$ ) from 0.3 to 0.5 m, no significant influence on ice loads was observed.

### The results of the geotechnical stability analysis

Soil parameters used in analysis are presented in Table 5. The results of the stability analysis for overturning and sliding are presented in Figure 8 and Table 6.

Based on the results of the gabion wall check for overturning and sliding, Table 6 shows the overall check results – the wall is satisfactory. The results of the stability analysis for bearing failure are presented in Table 7. Based on the results of the gabion wall check for overturning and sliding, Table 7 shows the overall verification results – bearing capacity of foundation (soil) is satisfactory. The results of deep-seated failure of the retained slope are presented in Table 8.

**Table 5.** Soil parameters

Sand with trace of fines (S-F), medium dense	
Unit weight	$\gamma = 17.50 \text{ kN}\cdot\text{m}^{-3}$
Stress-state	effective
Angle of internal friction	$\varphi_{\text{ef}} = 29.50^\circ$
Cohesion of soil	$c_{\text{ef}} = 0.00 \text{ kPa}$
Angle of friction between structure and soil	$\delta = 0.66^\circ$
Soil	cohesionless
Saturated unit weight	$\gamma_{\text{sat}} = 17.50 \text{ kN}\cdot\text{m}^{-3}$
Well graded sand (SW), medium dense	
Unit weight	$\gamma = 20.00 \text{ kN}\cdot\text{m}^{-3}$
Stress-state	effective
Angle of internal friction	$\varphi_{\text{ef}} = 36.50^\circ$
Cohesion of soil	$c_{\text{ef}} = 0.00 \text{ kPa}$
Angle of friction between structure and soil	$\delta = 0.66^\circ$
Soil	cohesionless
Saturated unit weight	$\gamma_{\text{sat}} = 20.00 \text{ kN}\cdot\text{m}^{-3}$

Source: own work.

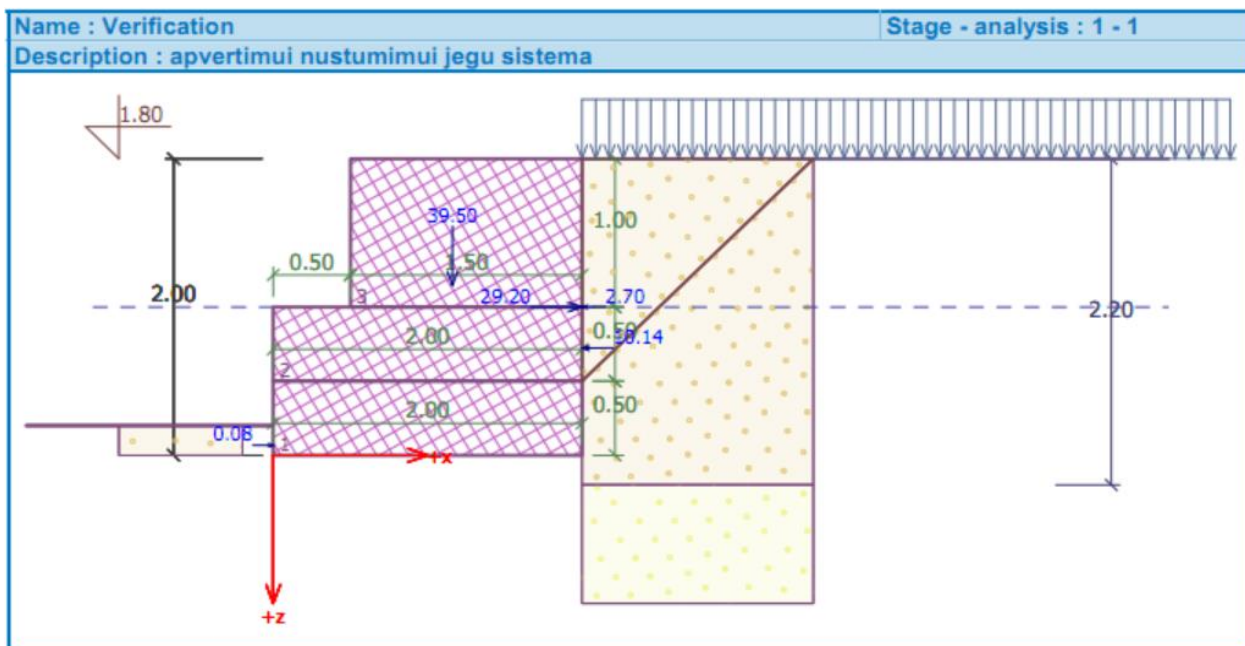


**Fig. 8.** The calculation scheme for verification of wall

Source: own work.

**Table 6.** The gabion wall check for overturning and sliding

Check for overturning stability		Check for slip	
Resisting moment ( $M_{res}$ )	53.91 kN·m <sup>-1</sup>	Resisting horizontal force ( $H_{res}$ )	20.42 kN·m <sup>-1</sup>
Overturning moment ( $M_{ovt}$ )	13.53 kN·m <sup>-1</sup>	Active horizontal force ( $H_{act}$ )	11.94 kN·m <sup>-1</sup>
Wall resistance against overturning is satisfactory		Wall resistance against slip is satisfactory	

Source: own work.

**Table 7.** The gabion wall stability analysis for bearing failure

Eccentricity verification		Verification of bearing capacity	
Norm, force 53.47 kN·m <sup>-1</sup>	Maximum eccentricity of normal force $e = 0.000$ Maximum allowable eccentricity $e_{alw} = 0.333$	Maximum stress at footing bottom $\sigma = 26.74$ kPa	Bearing capacity of foundation soil $R_d = 35.71$ kPa
Eccentricity of the normal force is satisfactory		Bearing capacity of foundation soil is satisfactory	

Source: own work.

**Table 8.** Slope stability verification (using Bishop method)

Forces		Moments	
Sum of active forces ( $F_a$ )	35.21 kN·m <sup>-1</sup>	Sliding moment ( $M_a$ )	151.74 kN·m <sup>-1</sup>
Sum of passive forces ( $F_p$ )	57.37 kN·m <sup>-1</sup>	Resisting moment ( $M_p$ )	247.25 kN·m <sup>-1</sup>

Source: own work.

Based on the results of the gabion wall check for slope stability verification, Table 8 shows that slope stability is acceptable – factor of safety ( $F_S$ ) = 1.63 > 1.50 (minimum required  $F_S$ ).

## CONCLUSIONS

1. The results of wave load calculation show that the gabion retaining wall for shore protection is subject to a horizontal projection of wave force ( $P_x$ ) equal to 6.13 kN·m<sup>-1</sup> and vertical projection of wave force ( $P_z$ ) equal to 7.72 kN·m<sup>-1</sup>. The magnitude of the calculated hydrodynamic forces shows the possible reason of the structural deformations and settlement of former reinforced concrete retaining wall.
2. Based on the results of the ice loading calculations, it has been found that:
  - The changes of ice thickness directly affect calculation results of all types of the ice loads.
  - The changes of average wind speed during the temperature drop ( $V_w$ ) have impact on values of horizontal linear loads on structures due to the ice cover thermal expansion effect ( $P_3$  or  $q$ ).
  - The changes of speed of ice field movement ( $v_l$ ) from 0.5 m·s<sup>-1</sup> to 1.5 m·s<sup>-1</sup> and ice field maximum area ( $A_l$ ) from 50 m<sup>2</sup> to 150 m<sup>2</sup> directly affect the calculation results of the horizontal load of moving ice fields on a structure with a vertical front edge ( $P_1$  or  $F_{b,w}$ ).
  - In the case of a change in water level ( $h_0$ ) from 0.3 m to 0.5 m, no significant influence on ice loads was observed. The calculated ice loads have direct impact on stability of the gabion retaining wall.
3. The numerical results reveal good geotechnical stability – calculations of the stability of a typical gabion retaining wall in case of overturning and sliding show that the wall resistance against overturning and slip is satisfactory. The evaluation of the gabion retaining wall base strength according to the loss of load-bearing capacity shows that the eccentricity of the normal force is satisfactory and the bearing capacity of foundation soil is satisfactory. Overall verification shows that the bearing

capacity of foundation (soil) is satisfactory. Calculations of the deep seated failure of the retained slope show that the slope stability is acceptable.

4. The results of wave and ice loads calculation and geotechnical stability analysis show that structures formed from gabions should be able to resist different types of loads and are suitable for protection of lake coastline.

## Authors' contributions

Conceptualisation: R.Š. and I.A.; methodology: R.Š. and R.B.; validation: R.Š., I.A. and K.G.; formal analysis: R.Š. and M.K.; investigation: R.Š.; resources: I.A. and M.K.; data curation: K.G. and M.K.; writing – original draft preparation: R.Š.; writing – review and editing: I.A. and M.K.; visualisation: K.G.; supervision: R.Š.

All authors have read and agreed to the published version of the manuscript.

## REFERENCES

- Chanson, H. (2015). Embankment overtopping protection systems. *Acta Geotechnica*, 10, 305–318. <https://doi.org/10.1007/s11440-014-0362-8>
- Cherkasova, L. (2019). Application of gabions for strengthening marine coastal slopes. *Journal of Physics: Conference Series*, 1425. <https://doi.org/10.1088/1742-6596/1425/1/012206>
- Chunjiang, L., Zhijun, L., Yu, Y., Qingkai, W., Baosen, Z. & Yu, D. [s.a.]. Theory and Application of Ice Thermodynamics and Mechanics for Natural Sinking of Gabion Mattress on Ice. <https://ssrn.com/abstract=4149366> [preprint, not reviewed].
- European Union [EU], (2004). Eurocode 7: Geotechnical design. Part 1: General rules (EN 1997-1) [Authority: The European Union Per Regulation 305/2011, Directive 98/34/EC, Directive 2004/18/EC].
- Fiske, J. (2014). Case Studies Highlight Marine Mattress Applications. *Geosynthetics*, 32.
- Hämmerling, M., Walczak, N., Walczak, Z. & Zawadzki, P. (2019). Ocena stanu technicznego umocnień brzegów cieków i zbiorników na terenie miasta Poznania [Assessment of technical conditions of bank protection of watercourses and reservoirs in the city of Poznań]. *Acta Scientiarum Polonorum. Formatio Circumi-*

- ectus*, 18 (3), 3–17. <http://doi.org/10.15576/ASP.FC/2019.18.3.3>
- Karambas, T. V. & Samaras, A. G. (2017). An Integrated Numerical Model for the Design of Coastal Protection Structures. *Journal of Marine Science and Engineering*, 5 (4), 50. <https://doi.org/10.3390/jmse5040050>
- Kawalec, J. J., Kwiecien, S., Pilipenko, A. & Rybak, J. (2017) Application of Crushed Concrete in Geotechnical Engineering – Selected Issues. *IOP Conference Series: Earth and Environmental Science*, 95 (2). <https://iopscience.iop.org/article/10.1088/1755-1315/95/2/022057>
- Kudale, M. D. & Bhalerao, A. R. (2015). Equivalent Monochromatic Wave Height for the Design of Coastal Rubblemound Structures. *Aquatic Procedia*, 4, 264–273. <https://doi.org/10.1016/j.aqpro.2015.02.036>
- Kudale, A. M., Kudale, M. D. & Kulkarni P. B. (2021). Roll of hydraulic modeling in predicting impact of coastal structures. *International Journal of Advanced Research in Engineering and Technology (IJARET)*, 12 (10), 48–60.
- Kurbanov, S., Sozaev, A., Shogenov, A. & Karshiev, A. (2021). Bioengineering systems for protection and improvement of urbanized areas of coastal and recreational zones. *E3S Web Conferences*, 262, 03021. <https://doi.org/10.1051/e3sconf/202126203021>
- Lietuvos Standartizacijos Departamentas (2004a). *Statybos techninis reglamentas Hidrotechnikos statiniai. Pagrindinės nuostatos [Hydraulic structures. Basic provisions]* (STR 2.02.06:2004). Vilnius.
- Lietuvos Standartizacijos Departamentas (2004b). *Statybos techninis reglamentas Hidrotechnikos statinių poveikiai ir apkrovos [Effects and loads on hydraulic structures]* (STR 2.05.15:2004). Vilnius.
- Lietuvos Standartizacijos Departamentas (2017). *Statybos techninis reglamentas Statinių klasifikavimas [Classification of structures]* (STR 1.01.03:2017). Vilnius.
- Luan, Y., Li, D., Chen, H., Geng, B. & Liu, H. (2020). Review of Ecological Coast Construction Technology. *International Conference on Intelligent Transportation, Big Data & Smart City (ICITBS)*, Vientiane, Laos, 2020, 181–186. <https://doi.org/10.1109/icitbs49701.2020.00045>
- Łabuz, T.A. (2015). Environmental Impacts – Coastal Erosion and Coastline Changes. In *The BACC II Author Team, Second Assessment of Climate Change for the Baltic Sea Basin*. (Part of the Regional Climate Studies, pp. 381–396). <https://doi.org/10.1007/978-3-319-16006-120>
- Möller, I. (2019) Applying Uncertain Science to Nature-Based Coastal Protection: Lessons From Shallow Wetland-Dominated Shores. *Frontiers in Environmental Science*. (Vol. 7:49). <https://doi.org/10.3389/fenvs.2019.00049>
- Razali, M. R., Hamzah, A. F., Othman, I. K., Lee, H. L., Rosli, N. S., Azhary, W. A. H. W. M., Ahmad, A., Hamzah, S. B. & Jamal, M. H. (2022). Potential Development of Coastal Reservoir in Malaysia. In S. Harun, I. K. Othman, M. H. Jamal (Eds) *Proceedings of the 5<sup>th</sup> International Conference on Water Resources (ICWR)* (Vol. 1. Lecture Notes in Civil Engineering, pp. 397–407). [https://doi.org/10.1007/978-981-19-5947-9\\_32](https://doi.org/10.1007/978-981-19-5947-9_32)
- Różyński, G. (2020). Parameterization of erosion vulnerability at coasts with multiple bars: a case study of Baltic Sea coastal segment in Poland. *Coastal Engineering*, 159. <https://doi.org/10.1016/j.coastaleng.2020.103723>
- Różyński, G. & Cerkowniak, R. (2022). Resilience of Coastal Lake Barriers in Poland in Light of Geological and Bathymetric Data and Hydrodynamic Simulations. *Frontiers in Marine Science. Coastal Ocean Processes*, 9. <https://doi.org/10.3389/fmars.2022.815405>
- Safari Ghaleh, R., Aminoroayaie Yamini, O., Mousavi, S. H. & Kavianpour, M. R. (2021). Numerical Modeling of Failure Mechanisms in Articulated Concrete Block Mattress as a Sustainable Coastal Protection Structure. *Sustainability*, 13, 12794. <https://doi.org/10.3390/su132212794>
- Sherlin, P. N. S., Sundaravadivelu, R. & Saha, N. (2018). Hydrodynamic and Geotechnical Stability of Geo-Tube and Gabion Armored Embankment. *OCEANS 2018 MTS/IEEE Charleston*. Charleston, SC, USA, 2018, 1–8. <https://doi.org/10.1109/oceans.2018.8604872>
- Smith, A. & Houser, C. (2022). Perspectives on Great Lakes coastal management: A case study of the Point Pelee foreland, Canada. *Ocean & Coastal Management*, 228. <https://doi.org/10.1016/j.ocecoaman.2022.106329>
- Sukhinov, A. I., Chistyakov, A. E. & Protsenko E. A. (2021). Coastal protection structures influence on diffraction and reflection of waves simulation based on 3D wave hydrodynamics model. *Journal of Physics: Conference Series*, 1902. <https://doi.org/10.1088/1742-6596/1902/1/012133>
- Toprak, B., Sevim, O. & Kalkan, I. (2016). Gabion Walls And Their Use. *International Journal of Advances in Mechanical and Civil Engineering*, 3 (4), 56–58.

## ZASTOSOWANIE GABIONÓW DO PROJEKTOWANIA KONSTRUKCJI OCHRONY WYBRZEŻA W JEZIORACH

### STRESZCZENIE

W wypadku zbiorników wodnych i jezior o dużych obszarach droga spływu fal jest również duża, co powoduje powstawanie wysokich fal w kierunku wiejącego wiatru. Fale te intensywnie niszczą brzeg jeziora lub zbiornika wodnego. Innym intensywnym czynnikiem erozji wybrzeża jest lód. Do ochrony wybrzeża zbiorników wodnych stosuje się wiele środków inżynierskich: w wypadku jezior są to płyty żelbetowe, bloki, wysięgniki, systemy komórkowe (geosyntetyki) itp. W niniejszej pracy przeanalizowano zerodowaną linię brzegową, przekształconą poprzez zainstalowanie konstrukcji zabezpieczającej wybrzeże z wykorzystaniem konstrukcji gabionowych. Gabiony są przeznaczone do ochrony brzegów i skarp przed szybkim spływem wody (prędkość wody powyżej  $5 \text{ m} \cdot \text{s}^{-1}$ ) oraz uderzeniami lodu. Projektuje się je według zasad geotechnicznych, oceniając stateczność zgodnie z granicznymi sytuacjami projektowymi określonymi w Eurokodzie 7 (EN 1997-1). Celem niniejszej pracy jest zilustrowanie przypadków obciążeń falami i lodem oraz geotechnicznych sytuacji projektowych, ocenianych w projekcie konstrukcji ochrony wybrzeża, która jest wykonana z gabionów.

**Słowa kluczowe:** struktury ochrony wybrzeża, fale i uderzenia lodu, gabiony, geotechniczne sytuacje projektowe